Coordination Stoichiometry Effects on the Binding Hierarchy of Histamine and Imidazole–M²⁺ Complexes

Jake Song,* Eesha Khare, Li Rao, Markus J Buehler, and Niels Holten-Andersen*

Histidine–M²⁺ coordination bonds are a recognized bond motif in biogenic materials with high hardness and extensibility, which has led to growing interest in their use in soft materials for mechanical function. However, the effect of different metal ions on the stability of the coordination complex remains poorly understood, complicating their implementation in metal-coordinated polymer materials. Herein, rheology experiments and density functional theory calculations are used to characterize the stability of coordination complexes and establish the binding hierarchy of histamine and imidazole with Ni²⁺, Cu²⁺, and Zn²⁺. It is found that the binding hierarchy is driven by the specific affinity of the metal ions to different coordination states, which can be macroscopically tuned by changing the metal-to-ligand stoichiometry of the metal-coordinated network. These findings facilitate the rational selection of metal ions for optimizing the mechanical properties of metal-coordinated materials.

J. Song, E. Khare, N. Holten-Andersen
Department of Materials Science and Engineering
Massachusetts Institute of Technology
77 Massachusetts Avenue, Cambridge, MA 02139, USA
E-mail: jakesong@mit.edu; nih221@lehigh.edu

E. Khare, M. J Buehler
Laboratory for Atomistic and Molecular Mechanics (LAMM)
Massachusetts Institute of Technology
77 Massachusetts Avenue, Cambridge, MA 02139, USA

L. Rao
Department of Chemistry
Central China Normal University
Wuhan 430079, P. R. China

M. J Buehler
Center for Computational Science and Engineering
Schwarzman College of Computing
Massachusetts Institute of Technology
77 Massachusetts Avenue, Cambridge, MA 02139, USA

N. Holten-Andersen
Department of Bioengineering and Department of Materials Science and Engineering
Lehigh University
27 Memorial Dr W, Bethlehem, PA 18015, USA

1. Introduction

Coordination interactions between transition metals ions and biomolecules have long been appreciated to be an essential component of biological function within living organisms, such as in the self-assembly of biological proteins[1–3] and transport and sequestration of ions and molecules.[4–6] More recently, there has been a growing appreciation of how these coordination interactions might facilitate load-bearing ability in biogenic materials.[7] For instance, marine mussels are known to incorporate metal ions into cuticles to produce high hardness and extensibility,[8] properties that are often diametric in synthetic materials. Marine worms also incorporate metal-coordination crosslinks in their hard, condensed mandibular structure.[9–11]

One example of biological metal coordination is the coordination interaction between histidine and common transition metals such as nickel (Ni²⁺), zinc (Zn²⁺), and copper (Cu²⁺), which has been implicated to facilitate diverse mechanical behavior ranging from hardness in the jaws of the *Glycera* and *Nereis* to energy dissipation in the byssal threads of the *Mytilus* (**Figure 1**A).[9,10,12–16] Accordingly, there has been growing interest[17] in utilizing the interactions between common biogenic transition metals and histidine (or imidazole, the functional group in histidine) as crosslinkers in synthetic materials, such as in polymer materials[18–23] and histidine-rich protein-based materials.[24–26]

Despite this growing application of histidine–metal-ion (M²⁺) interactions in synthetic soft materials, there is an unresolved understanding of the molecular origins of the different dissociation rates exhibited by histidine motifs crosslinked with Ni²⁺, Zn²⁺, and Cu²⁺ ions in these materials. A complicating factor in understanding the "hierarchy" of binding between histidine (and related ligands such as histamine and imidazole) and these transition metals is that the hierarchy appears to be strongly system or configuration dependent. For instance, the relaxation times of polymer networks crosslinked by coordination between histamine and Ni²⁺, Zn²⁺, and Cu²⁺ ions follows a hierarchy of Ni²⁺ > Cu²⁺ > Zn²⁺,[18,19] and the same order is observed in polymer melts crosslinked by acetate ligands and the same metals.[27] This behavior is contrasted by the mechanical reinforcement of synthetic hydrogels with imidazole-rich protein residues; the modulus of these imidazole-rich protein networks crosslinked with transition metal ions show Zn²⁺ > Ni²⁺ for polymer networks with imidazole-rich coiled-coil crosslinking motifs,[24,25] and also

ADVANCED
SCIENCE NEWS
www.advancedsciencenews.com

[M] acro-
molecular
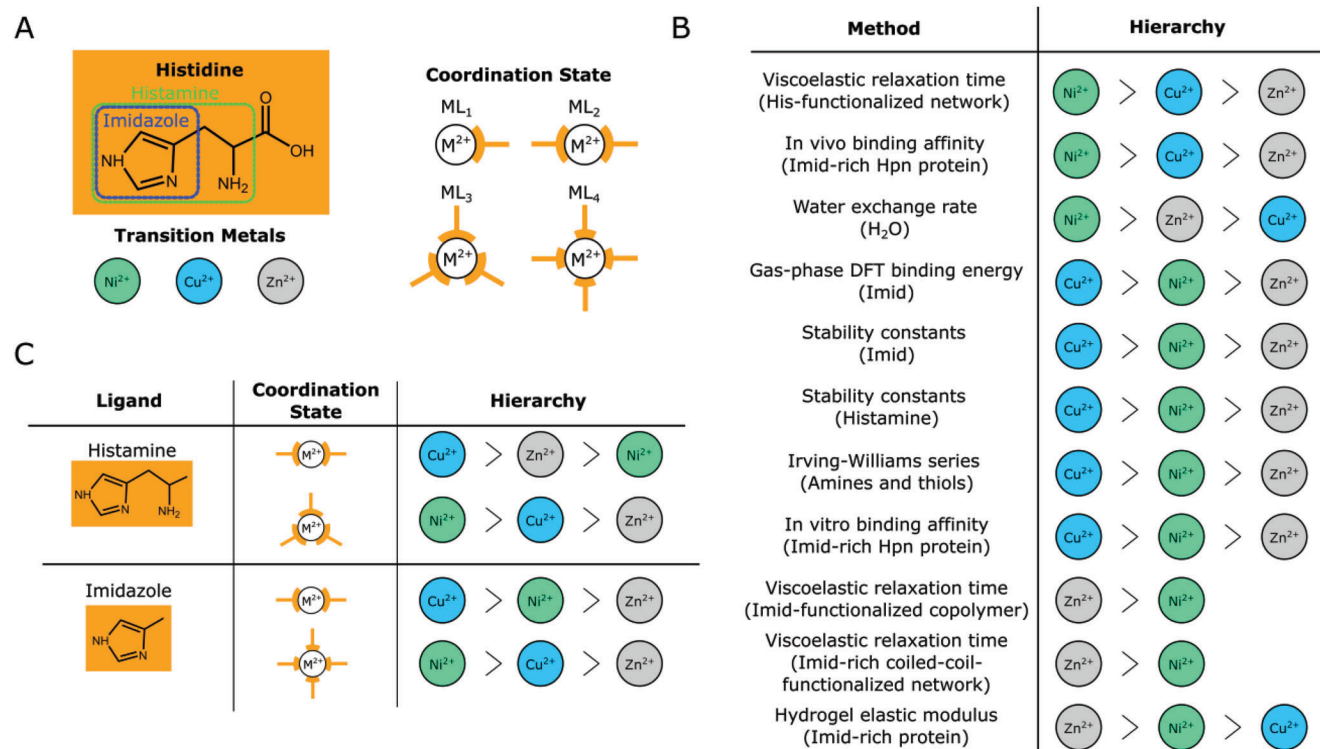Rapid Communications
www.mrc-journal.de

Figure 1. Diverse binding hierarchy between histidine and Ni^{2+}, Cu^{2+}, and Zn^{2+}. A) Structure of histidine and its related functional groups histamine and imidazole. These histidine groups form complexes of various coordination numbers with first-row transition metals such as Ni^{2+}, Cu^{2+}, and Zn^{2+}. B) Reported binding hierarchy of Ni^{2+}, Cu^{2+}, and Zn^{2+} with histidine-containing materials and related systems. C) Results from this study for the binding hierarchy of histamine and imidazole with Ni^{2+}, Cu^{2+}, and Zn^{2+} at different coordination states.

for acrylamide copolymer networks with imidazole functional groups.[28] A similar trend of $Zn^{2+} > Ni^{2+} > Cu^{2+}$ is also observed in the case of hydrogels made with imidazole-rich *Nvjp-1* protein found in the jaws of the marine sandworm *Nereis*.[26]

A hypothesis to explain the apparent discrepancy in the metal ion hierarchy between histamine-containing synthetic materials and imidazole-rich protein residues is that both nitrogen atoms in the histamine ligand are available for coordination interactions with M^{2+} in synthetic materials, whereas only one nitrogen atom in the imidazole ligand is available coordination interactions in protein systems where the carboxyl and amine groups form the backbone of the protein. However, the cumulative binding stability constants of imidazole and histamine with M^{2+} follows a hierarchy of $Cu^{2+} > Ni^{2+} > Zn^{2+}$,[29] as does DFT calculation results of the interaction between a single imidazole ligand and M^{2+}.[30] The $Cu^{2+} > Ni^{2+} > Zn^{2+}$ hierarchy is also predicted by the Irving-Williams series, which ranks the stability of octahedral complexes of amines and thiols with first-row transition metal ions.[31] This relative ordering is in contrast with the hierarchy presented above for histamine-rich networks and imidazole-rich proteins. In addition, in vitro binding affinities of these transition metals with imidazole-rich Hpn proteins and in vivo selectivity of *Helicobacter pylori* which use Hpn proteins to sequester transition metal ions show different hierarchies of $Cu^{2+} > Ni^{2+} > Zn^{2+}$ and $Ni^{2+} > Cu^{2+} > Zn^{2+}$, respectively.[6] The exchange time of H_2O with these three transition metals, which is yet another measure of the dissociation rates of bound species to the

metal ions, follow an order of $Ni^{2+} > Zn^{2+} > Cu^{2+}$. Thus, the reported binding hierarchies of imidazole–M^{2+} interactions are prevalently system-specific (Figure 1B). It is worth noting that each of these results measure different aspects of binding between the transition metals and the ligands: the stability constant, binding affinity, and elastic modulus measurements are a measure of the overall thermodynamic stability of the coordination complex, while the viscoelasticity and ligand exchange studies are a measure of the overall kinetic stability of the coordination complex. Furthermore, the mechanical measurements (elasticity and viscoelasticity) only provide information on the binding affinity of higher coordination states, as monocoordinated species do not provide mechanical reinforcements in these systems. However, it is apparent that system-specific metal hierarchies are observed even with these metrics in mind, posing the question as to the origins of these literature observations.

We suggest that developing an understanding of the binding hierarchy of imidazole with M^{2+} ions must begin with an assessment of the affinity of the imidazole–M^{2+} interaction in an ideal environment in which the coordination interactions are not affected by other features of the system. An example of a nonideal environment might be the conformational restrictions on the imidazole–M^{2+} interactions in biological systems due to the structural self-assembly of the protein strands. Thus, here we aim to study the binding hierarchy of histidine and imidazole with M^{2+} ions by utilizing a flexible telechelic polymer hydrogel as the model system. In this configuration, the telechelic end groups
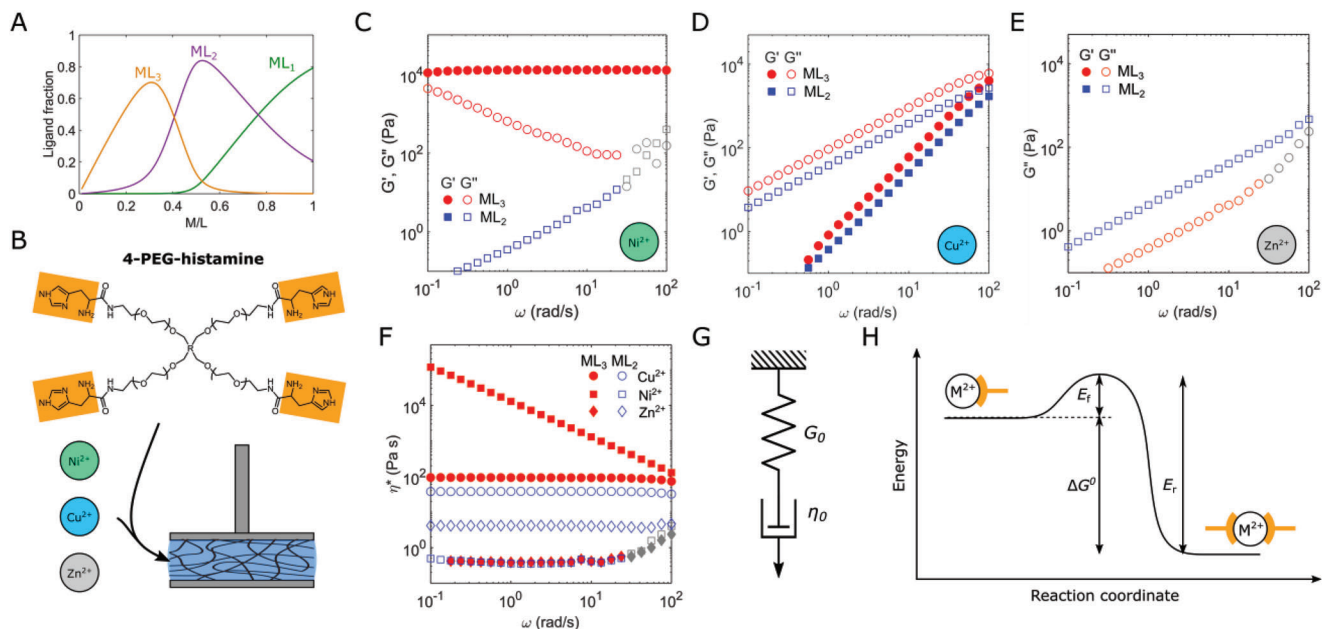
2300077 (2 of 8)

Figure 2. Coordination-number-dependent viscoelasticity of a histamine-functionalized polymer network. A) Speciation analysis of histamine with Ni^{2+}. Controlling the stoichiometric ratio of metal ions to ligands changes the population of ML_1-, ML_2-, and ML_3-coordinated species in the system. B) Structure of 4-PEG-histamine which is mixed with M^{2+} ions under stoichiometrically controlled conditions to design viscoelastic fluids, which are then measured on a rheometer. C–E) Small-amplitude oscillatory shear analysis ($T = 5\ °C$) of 4-PEG-histamine with Cu^{2+}, Ni^{2+}, and Zn^{2+} at ML_3 and ML_2 coordination numbers, and F) its representation in terms of a complex shear viscosity. Data below the inertial limit of the rheometer is colored in gray. G) Schematic illustration of the Maxwell model of linear viscoelasticity, represented by a spring (with a spring constant G_0) and a dashpot (with a viscosity η_0) in series. H) Schematic illustration of the reaction coordinate underlying a spontaneous metal-coordination event.

of the polymers can be functionalized with either histamine or imidazole to induce transient crosslinking with Ni^{2+}, Zn^{2+}, and Cu^{2+} ions. The binding affinity between the ligands and the M^{2+} can thus be studied by monitoring the viscoelasticity of the hydrogel network, as the dissociation kinetics of such structures govern the relaxation of the hydrogel network.[32] Furthermore, this configuration allows control of the stoichiometric ratio of histidine and M^{2+}, which provides an easy handle for controlling the metal–ligand coordination number (ML_1, ML_2, ML_3, and ML_4).[20,33]

Thus, here we characterize the viscoelasticity of transient networks formed with histamine or imidazole and Ni^{2+}, Zn^{2+}, and Cu^{2+} ions under different stoichiometric conditions and complement this effort with a density functional theory (DFT) investigation of the overall affinity of complexes at different coordination numbers. Our characterization shows that the hierarchy of Ni^{2+}, Zn^{2+}, and Cu^{2+} binding stability is dramatically affected by the coordination number of the metal–ligand interaction (Figure 1C) and provides a structural explanation of the binding hierarchy.

2. Results

The speciation of metal–ligand complexes is driven by the stoichiometric quantities of the metal ions and ligands in the reaction media. This is illustrated by a speciation analysis of Ni^{2+} and histamine (see SI Methods), which has also been demonstrated in recent work[20] (**Figure 2**A). This example analysis shows that the dominant coordination number of the metal–ligand complexes in the reaction media is strongly stoichiometry-dependent, such

that the metal–ligand ratio can be adjusted to preferentially form *mono*, *bis*, or *tris* coordination complexes. The manipulation of the coordination number via the reaction media stoichiometry will in turn significantly affect the structure and stability of the complexes, which we aim to characterize in this work.

To do so, we begin with a rheological characterization of the dynamics of reversible polymer networks with histamine–M^{2+} complexes of different coordination numbers. We adopt a variation of the approach of Grindy et al., in which histamine-functionalized 4-arm poly(ethylene glycol) (4-PEG-histamine) with Ni^{2+} was used to study the viscoelasticity of polymer networks under different histamine–Ni^{2+} stoichiometries.[20] In our study, we investigate the metal–ligand stoichiometry-dependent rheological properties of 4-PEG-histamine and M^{2+} networks buffered with MOPS, which is a Good's buffer at physiological pH that shows minimal interaction with transition metals such as Cu^{2+}, Ni^{2+}, and Zn^{2+} and is thus used as standard buffers in binding assays.[38–40] This is in contrast to the previous study[20] in which the gels buffered by phosphate-buffered saline (PBS), where PO_4^- groups in PBS can interact significantly with the M^{2+}. The use of PBS can therefore pose complications in studying the stability of the resulting coordination complexes, especially since interaction between M^{2+} and anionic species can cause a change in the coordination number of the metal centers.[26]

The storage modulus $G'(\omega)$ and loss modulus $G''(\omega)$ of 4-PEG-histamine–M^{2+} networks using different stoichiometries are shown in Figure 2C–E ($T = 5\ °C$). The networks exhibit Maxwell-like viscoelastic behavior, as expected based on prior

ADVANCED
SCIENCE NEWS
www.advancedsciencenews.com

[M] acro-
molecular
Rapid Communications
www.mrc-journal.de

results[18,19] and as expected of transient networks.[41,42] In the ML$_3$-coordinated networks with Ni^{2+}, Cu^{2+}, and Zn^{2+}, we observe an ordering of the dissociation times of the 4-PEG network, indicated by the crossover time $\tau_c = 1/\omega_c$, to be Ni^{2+} > Cu^{2+} > Zn^{2+} in agreement with refs. [18, 19]. However, this trend is completely different in a network formed with an ML$_2$ metal–ligand coordination. We find that the Ni^{2+} network completely loses its ability to form a viscoelastic network as indicated by the purely viscous response of the network. The Cu^{2+} network becomes slightly weaker, indicated by the slight lowering of the viscoelastic moduli of the network. The Zn^{2+} network becomes slightly more viscous, as indicated by an increase in $G''(\omega)$. Comparing just the complex shear viscosity $\eta^*(\omega) = G^*(\omega)/\omega$ of these networks (which is a measure of the zero-shear viscosity (η_0) of the network via the Cox–Merz rule), we find that for ML$_2$ stoichiometric conditions, the ordering of dissociation times is Cu^{2+} > Zn^{2+} > Ni^{2+} (Figure 2F).

For a system following the Maxwell model of viscoelasticity (Figure 2G), the zero-shear viscosity η_0 of a material is a function of the network elasticity G_0 and the characteristic crossover time τ_c, such that $\eta_0 = G_0\tau_c$. Here, we can recognize that G_0 depends on the density of crosslinks in the network (ρ)[43] and that τ_c depends both on the dissociation rate (k_d) of the crosslinks as well as ρ.[41,42] Thus, we can surmise that η_0 in our network is dependent on both ρ and k_d of the crosslinking interactions. ρ is a quantity related to the static equilibrium concentration of the crosslinks, and thus related to the stability constant K, which is a measure of the *thermodynamic* free energy change ΔG^0 of the forward binding process between the metals and the histamine ligands. In contrast, k_d is a measure of the *kinetic* activation energy of the reverse binding process, E_r (Figure 2H).

We cannot decouple the contributions of G_0 and τ_c on the η_0 of the material, since the crosslinker dynamics for the polymer networks (except the Ni^{2+}His$_3$ networks) are too fast for ω_c to be measurable on the rheometer even at $T = 5\,^\circ$C. Thus, we are not able to decouple the hierarchies of thermodynamic affinity and kinetic stability of the different histamine–M^{2+} complexes which give rise to the different dissociation times. Nevertheless, we hypothesize that the observed η_0 is dominated by the thermodynamic affinity of the histamine–M^{2+} complexes (i.e., ΔG^0 in Figure 2H). This is because the binding of histamine with these transition metals is spontaneous[44] and occurs within seconds, evidenced by the rapid gelation of the system. Since the forward reaction is rapid, the forward activation energy E_f should be small, and thus we expect ΔG^0 to be similar to the reverse activation energy E_r (or at the very least, scale in a similar manner).

Thus, the experimental data indicates that there is a coordination number-dependent hierarchy of thermodynamic affinity between histamine and Ni^{2+}, Cu^{2+}, and Zn^{2+}, where the ordering follows Ni^{2+} > Cu^{2+} > Zn^{2+} in an ML$_3$ configuration but the ordering changes to Cu^{2+} > Zn^{2+} > Ni^{2+} in an ML$_2$ configuration. While these results provide some clarity on the different contexts in which Ni^{2+} and Cu^{2+} provide the strongest binding to histamine, we recognize that these results cannot be easily compared to results from biological systems. This is because the amine group of the histamine amino acid is incorporated into the backbone of proteins and peptides, and thus it is rarely involved in metal-coordination interactions in metalloproteins,[45] except in a few some cases with Cu^{2+} or Cd^{2+}.[45–47] When the amine group cannot participate in the metal coordination, the binding of histamine groups with M^{2+} species are likely to be dominated by the interaction with coordinating nitrogen atoms on imidazole.[45] Thus, a more suitable comparison to binding hierarchy exhibited in biological systems may come from studying the hierarchy of imidazole–M^{2+} binding affinity. We thus perform a repeat of our experimental characterization of the complex shear viscosity η^* with 4-PEG-imidazole–M^{2+} networks (**Figure 3**). We study the dynamics of polymer networks formed under ML$_2$ and ML$_4$ imidazole–M^{2+} coordination stoichiometry, as metalloproteins rarely have more than four coordinated histidine amino acids unless there are two metals in the metal binding site.[42] For ML$_4$ coordination, a Ni^{2+} > Cu^{2+} > Zn^{2+} hierarchy of binding affinity is observed, while for ML$_2$ coordination, a Cu^{2+} > Ni^{2+} > Zn^{2+} hierarchy is observed (Figure 3B–D). A summary of the experimentally observed binding hierarchies of histamine and imidazole with Ni^{2+}, Cu^{2+}, and Zn^{2+} are illustrated in Figure 3E,F.

To validate these experimental results, we perform DFT calculations to determine ΔG^0 of ligand-M^{2+} coordination interaction in stepwise manner beginning with an ML$_1$ binding state (SI Methods). Each metal ion starts with binding six explicit water molecules in an octahedral arrangement as M(H$_2$O)$_6$. Histamine or imidazole ligands are sequentially added while displacing two or one water molecules respectively. The energy for each ML, ML$_2$, ML$_3$, and ML$_4$ complex is computed as a sum of the ligand addition steps to reach the required binding coordination number. The results of the calculations for histamine (Figure 4B) and imidazole (Figure 4C) for the different M^{2+} were in good agreement with the hierarchy obtained via viscosity measurements (Figure 3E,F). For histamine, experiments and computation show that ML$_3$ complexes follow a Ni^{2+} > Cu^{2+} > Zn^{2+} hierarchy, and ML$_2$ complexes follow a Cu^{2+} > Zn^{2+} > Ni^{2+} hierarchy. For imidazole, experiments and computation show that ML$_4$ complexes follow a Ni^{2+} > Cu^{2+} > Zn^{2+} hierarchy, and ML$_2$ complexes follow a Cu^{2+} > Ni^{2+} > Zn^{2+} hierarchy.

The DFT simulations also reveal the geometry of the metal-coordination complexes, which can provide insight into the structural origins of the binding hierarchy exhibited by the metals (Figure 4A). The identified coordination geometries of the complexes are generally in agreement with coordination geometries found in other work. For histamine complexes, Cu^{2+} and Zn^{2+} have been reported to undergo ML$_2$ coordination through square-pyramidal[48] and tetrahedral[49,50] structures, respectively, while Ni^{2+} is reported to undergo ML$_2$ and ML$_3$ coordination with histamine through an octahedral structure.[51–53] For imidazole complexes, Cu^{2+} has been reported undergo ML$_4$ or ML$_6$ coordination in square planar or octahedral geometries,[54–56] and Ni^{2+} and Zn^{2+} have been reported to undergo ML$_4$ coordination in a tetrahedral structure,[57] though the coordination number can be lower in biological protein systems due to metal ion interactions with other coordinating amino acids or water.[45,48,58]

The lowest energy structures from DFT (Figure 4a) can lend some insight into how the coordination geometries may influence binding hierarchies of the different transition metals. Ni^{2+} is found to preferentially bind in an octahedral geometry, whereas Cu^{2+} and Zn^{2+} are shown to preferentially bind in square planar or tetrahedral geometries.[59,60] These preferential bindings may explain the higher stability of histamine with Ni^{2+} compared to

**ADVANCED
SCIENCE NEWS**

www.advancedsciencenews.com

**{M}acro-
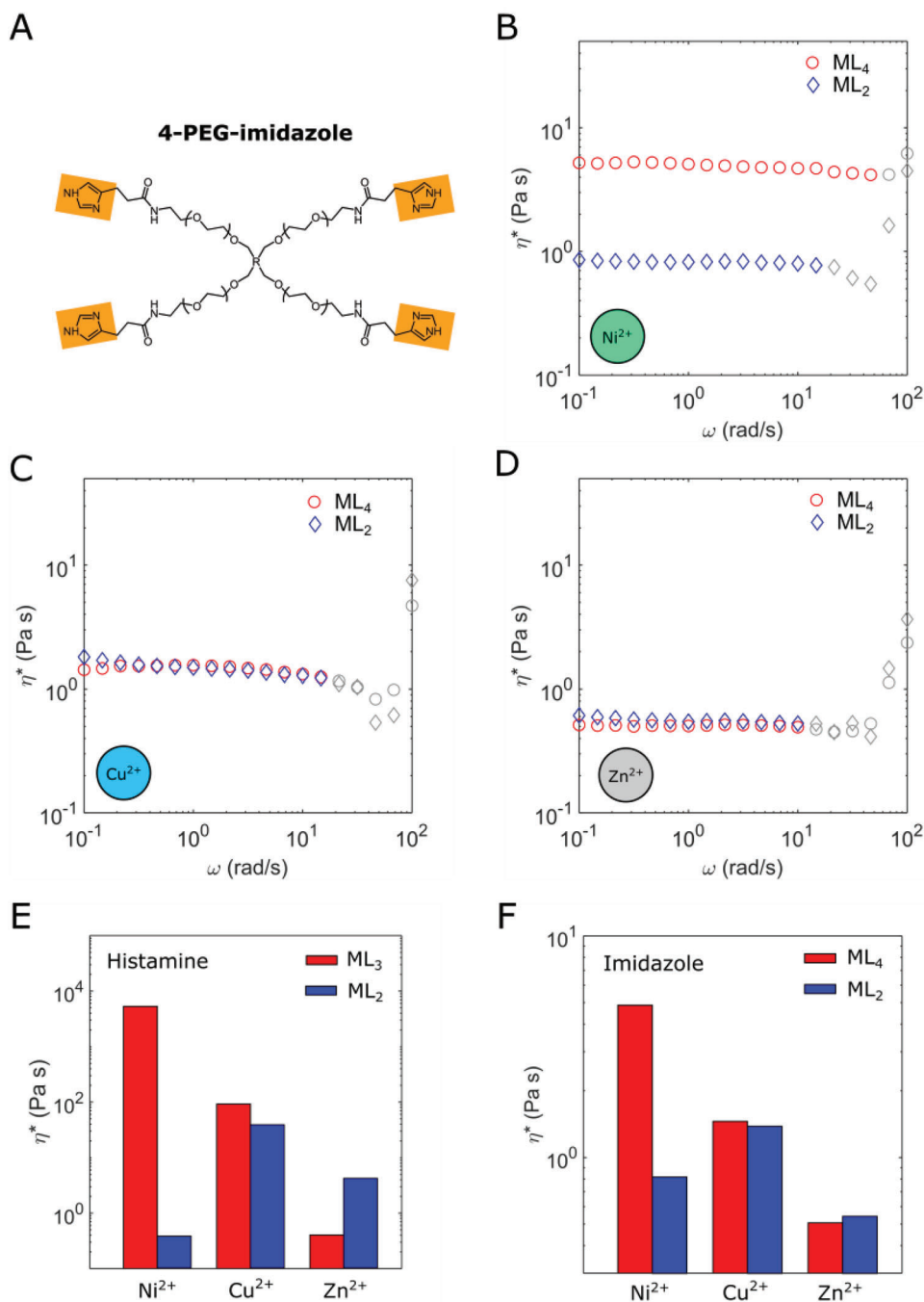molecular
Rapid Communications**

www.mrc-journal.de

Figure 3. Coordination-number-dependent viscosity of an imidazole-functionalized polymer network. A) Structure of 4-PEG-imidazole. B–D) Complex shear viscosity $\eta*$ measured via small-amplitude oscillatory shear experiments ($T = 5$ °C) on polymer networks mixed with Cu^{2+}, Ni^{2+}, and Zn^{2+} under stoichiometrically controlled conditions. Data below the inertial limit of the rheometer is colored in grey. E,F) Complex shear viscosity $\eta*$ of histamine- and imidazole-functionalized polymer networks with different coordination numbers.

the Cu^{2+} and Zn^{2+} in the ML_3 complex, and the higher stability of histamine with Cu^{2+} and Zn^{2+} compared to Ni^{2+} in the ML_2 complex. This explanation does not explain the high ML_4 stability of imidazole with Ni^{2+} compared to Cu^{2+} and Zn^{2+}, and high ML_2 stability of imidazole with Ni^{2+} compared to Zn^2. In our calculations, we find that octahedral coordination is not preferred by imidazole ML_4 complexes due to the steric crowding of imidazole

in octahedral geometries in the presence of water, and find that imidazole with Ni^{2+} shows a higher stability than Cu^{2+} and Zn^{2+} in the ML_4 complex, even though imidazole ML_4 is in a tetrahedral geometry. This might reflect the limitations of a purely structural perspective on the binding hierarchies, and the energetics of binding may also play a role in the binding hierarchy of the metal ions. For instance, the strong preference of imidazole
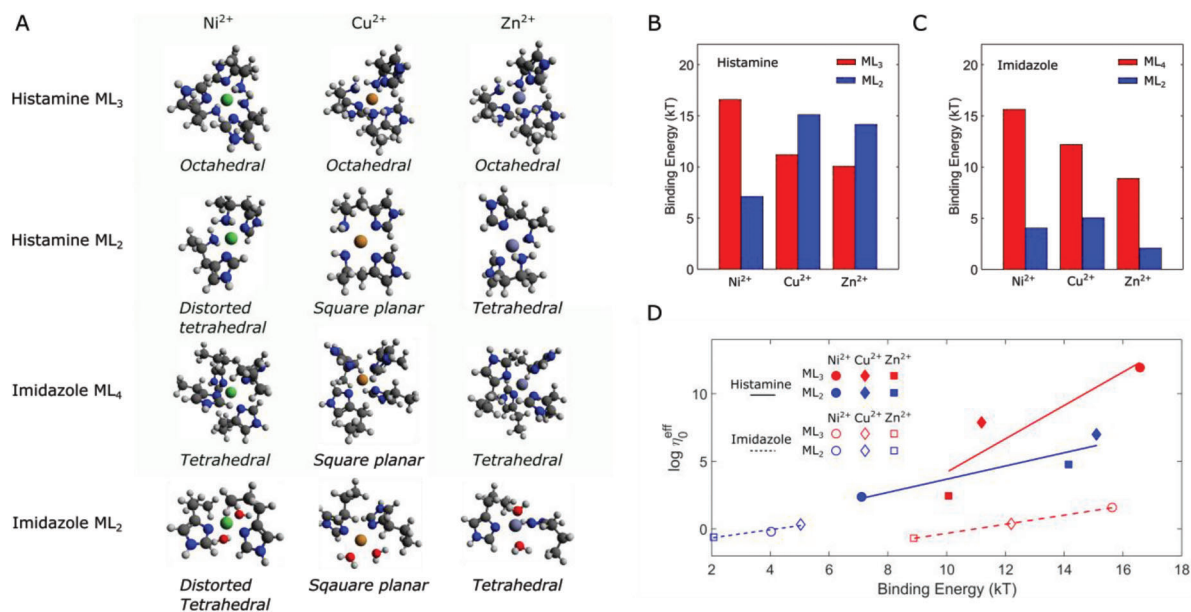
ADVANCED
SCIENCE NEWS

www.advancedsciencenews.com

{M} acro-
molecular
Rapid Communications

www.mrc-journal.de

Figure 4. Density functional theory (DFT) calculations of the binding hierarchy of histamine and imidazole with Ni^{2+}, Cu^{2+}, and Zn^{2+} under different coordination states. A) Equilibrated structures of the histamine and imidazole with Ni^{2+} (green), Cu^{2+} (orange), and Zn^{2+} (purple) as computed by DFT. Structures are identified by visual observation. B,C) Binding energy calculations for histamine and imidazole with different coordination numbers. The results are summarized in Figure 1C, D). Normalized viscosity η_0^{eff} (viscosity values in Figure 3E,F, normalized by η_0 of the 4-PEG-histamine and 4-PEG-imidazole polymer solutions without ions) versus the binding energies obtained from DFT calculations for histamine in ML_3 and ML_2 complexes, and imidazole in ML_4 and ML_2 complexes for Ni^{2+}, Cu^{2+}, and Zn^{2+}. The lines (solid for histamine, dashed for imidazole) serve as a guide to the eye.

to Ni^{2+} could be explained using crystal field theory, which evaluates the net stabilization of electrons in the d orbitals of metal ions depending on specific ligand field geometry. From Ni^{2+} (d^8) to Cu^{2+} (d^9) and Zn^{2+} (d^{10}), the incremental electrons would occupy the T_{2g} orbitals with higher energy, thus destabilizing the coordination compound.[61]

A more quantitative comparison of the experimental and computational results is shown in Figure 4D, where η_0^{eff} (which is the measured viscosity values normalized by η_0 of the 4-PEG-histamine and 4-PEG-imidazole polymer solutions without ions) is compared with the binding energy calculations. As expected, a positive correlation between binding energy (ΔG^0) and η_0^{eff} exists, though the correlation appears to be system-specific. For example, we see that the viscosities of the ML_4-coordinated 4-PEG-imidazole networks are only marginally higher compared to the ML_4-coordinated 4-PEG-imidazole networks, despite the substantial difference in the binding energies of the two coordination states. A possible hypothesis for this might be that the weak and dynamic coordination between imidazole and M^{2+} species may not fully prevent the precipitation of $M(OH)_2$ species, resulting in an overall lower population of M^{2+} species especially in the ML_2 state. We also cannot neglect the fact that the simulations do not consider any of the counter-ions present in the experimental system such as the MOPS buffer, and that some quantitative differences may arise as a result.

3. Discussion

We summarize our results in Figure 1C. Altogether, these results reveal a strong metal–ligand coordination number dependence on the thermodynamic binding affinity of imidazole and histamine–M^{2+} complexes, in which the hierarchy of binding affinities are dictated by the coordination number of the complexes formed under different stoichiometric conditions. This hierarchy is particularly driven by the tendency of Ni^{2+} to form ML_3 or ML_4 complexes with histamine and imidazole, respectively, suggesting that Ni^{2+} binding dictates in systems where the formation of complexes with larger coordination numbers is allowed, whereas Cu^{2+} binding dictates in systems where primarily *bis* complexes are formed. This might provide insight into the preferred binding state of histidine–M^{2+} complexes in biological systems; for instance, the in vivo binding of M^{2+} in *H. pylori* in which Ni^{2+} dominates the metal-binding hierarchy may be a result of the stoichiometric binding of the transition metals with histamine or imidazole in a ratio greater than 2 (i.e., ML_3 or higher), whereas the in vitro binding may be dominated by ML_2 complexes in which Cu^{2+} exhibits the greatest affinity to histamine or imidazole.

Our results are relevant in conditions in which histamine or imidazole ligands freely and exclusively bind to the M^{2+} at a neutral pH; deviations from these predictions can occur in the presence of competing species in non-buffered conditions that may compete with the M^{2+} binding, such as counterions[26] and hydroxides,[62] or in systems that exhibit higher-order self-assembly (for instance clustering of the metal–ligand complex).[24,25] For instance, this higher-order clustering of the coordination complexes is reported to occur in imidazole-containing polymer systems reinforced by Zn^{2+}, which can give rise to multivalent crosslinking and thus a slower mode of viscoelastic relaxation in these systems.[25] This may explain the substantially higher reinforcement of viscoelasticity in

**ADVANCED
SCIENCE NEWS**

www.advancedsciencenews.com

**macro-
molecular
Rapid Communications**

www.mrc-journal.de

imidazole-containing polymers by Zn^{2+} than other M^{2+} ions. The aggregate formation by Zn^{2+} is a noteworthy behavior—perhaps attributable to the formation of well-controlled tetrahedral coordination structures—which warrants future studies.

4. Conclusion

In conclusion, we have presented a combined experimental and computational study of the kinetic stability of histamine–M^{2+} and imidazole–M^{2+} complexes in their energetically preferred coordination structures. We first presented rheological characterizations of the dynamics of histamine- and imidazole-functionalized polymer networks which are transiently crosslinked by first row M^{2+}, and found a hierarchy of kinetic stability in different metals which are governed by the metal–ligand coordination state. We then verified these findings through DFT characterizations of the binding energy of histamine–M^{2+} and imidazole–M^{2+} complexes, finding that the kinetic stability of histamine–M^{2+} and imidazole–M^{2+} complexes are driven by the energetic stability of the complexes at different coordination numbers. We believe that these results provide a starting point for understanding the origins of the different binding hierarchy in histidine-rich systems reported in literature, and also for designing mechanically robust bio-mimetic soft materials using histidine complexes. Extending the study to account for metal–ligand coordination in more complex scenarios, such as in the presence of competitive species, would be an important extension of the study.

Supporting Information

Supporting Information is available from the Wiley Online Library or from the author.

Conflict of Interest

The authors declare no conflict of interest.

Data Availability Statement

The data that support the findings of this study are available from the corresponding author upon reasonable request.

[1] A. N. Istrate, S. A. Kozin, S. S. Zhokhov, A. B. Mantsyzov, O. I. Kechko, A. Pastore, A. A. Makarov, V. I. Polshakov, *Sci. Rep.* **2016**, *6*, 21734.

[2] J. A. Tainer, V. A. Roberts, E. D. Getzoff, *Curr. Opin. Biotechnol.* **1991**, *2*, 582.

[3] R. Zou, Q. Wang, J. Wu, J. Wu, C. Schmuck, H. Tian, *Chem. Soc. Rev.* **2015**, *44*, 5200.

[4] M. F. Perutz, *Annu. Rev. Biochem.* **1979**, *48*, 327.

[5] U. Krämer, J. D. Cotter-Howells, J. M. Charnock, A. J. M. Baker, J. A. C. Smith, *Nature* **1996**, *379*, 635.

[6] R. Ge, Y. Zhang, X. Sun, R. M. Watt, Q. Y. He, J. D. Huang, D. E. Wilcox, H. Sun, *J. Am. Chem. Soc.* **2006**, *128*, 11330.

[7] E. Degtyar, M. J. Harrington, Y. Politi, P. Fratzl, *Angew. Chem., Int. Ed.* **2014**, *53*, 12026.

[8] M. J. Harrington, A. Masic, N. Holten-Andersen, J. H. Waite, P. Fratzl, *Science* **2010**, *328*, 216.

[9] C. C. Broomell, M. A. Mattoni, F. W. Zok, J. H. Waite, *J. Exp. Biol.* **2006**, *209*, 3219.

[10] H. C. Lichtenegger, T. Schöberl, J. T. Ruokolainen, J. O. Cross, S. M. Heald, H. Birkedal, J. H. Waite, G. D. Stucky, *Proc. Natl. Acad. Sci. U. S. A.* **2003**, *100*, 9144.

[11] H. C. Lichtenegger, T. Schoberl, M. H. Bartl, H. Waite, G. D. Stucky, *Science* **2002**, *298*, 389.

[12] C. C. Broomell, S. F. Chase, T. Laue, J. H. Waite, *Biomacromolecules* **2008**, *9*, 1669.

[13] H. Birkedal, R. K. Khan, N. Slack, C. C. Broomell, H. C. Lichtenegger, F. Zok, G. D. Stucky, J. H. Waite, *ChemBioChem* **2006**, *7*, 1392.

[14] C. C. Broomell, F. W. Zok, J. H. Waite, *Acta Biomater.* **2008**, *4*, 2045.

[15] M. J. Harrington, J. H. Waite, *J. Exp. Biol.* **2007**, *210*, 4307.

[16] H. Zhao, J. H. Waite, *Biochemistry* **2006**, *45*, 14223.

[17] E. Khare, N. Holten-Andersen, M. J. Buehler, *Nat. Rev. Mater.* **2021**, *6*, 421.

[18] D. E. Fullenkamp, L. He, D. G. Barrett, W. R. Burghardt, P. B. Messersmith, *Macromolecules* **2013**, *46*, 1167.

[19] S. C. Grindy, R. Learsch, D. Mozhdehi, J. Cheng, D. G. Barrett, Z. Guan, P. B. Messersmith, N. Holten-Andersen, *Nat. Mater.* **2015**, *14*, 1210.

[20] S. C. Grindy, M. Lenz, N. Holten-Andersen, *Macromolecules* **2016**, *49*, 8306.

[21] G. E. Sanoja, N. S. Schauser, J. M. Bartels, C. M. Evans, M. E. Helgeson, R. Seshadri, R. A. Segalman, *Macromolecules* **2018**, *51*, 2017.

[22] J. D. Moon, R. Sujanani, Z. Geng, B. D. Freeman, R. A. Segalman, C. J. Hawker, *Macromolecules* **2021**, *54*, 866.

[23] S. Zechel, M. Hager, T. Priemel, M. Harrington, *Biomimetics* **2019**, *4*, 20.

[24] I. Tunn, A. S. De Léon, K. G. Blank, M. J. Harrington, *Nanoscale* **2018**, *10*, 22725.

[25] I. Tunn, M. J. Harrington, K. G. Blank, *Biomimetics* **2019**, *4*, 25.

[26] M. K. Gupta, K. A. Becknell, M. G. Crosby, N. M. Bedford, J. Wright, P. B. Dennis, R. R. Naik, *ACS Appl. Mater. Interfaces* **2018**, *10*, 31928.

[27] X. Zhang, Y. Vidavsky, S. Aharonovich, S. J. Yang, M. R. Buche, C. E. Diesendruck, M. N. Silberstein, *Soft Matter* **2020**, *16*, 8591.

[28] J. Zhao, T. Narita, C. Creton, *Adv. Polym. Sci.* **2020**, *285*, 1.

[29] R. M. Smith, A. E. Martell, *Critical Stability Constants*, , Plenum press, New York and London, **1976**, *2*.

[30] G. M. Ross, I. L. Shamovsky, S. B. Woo, J. I. Post, P. N. Vrkljan, G. Lawrance, M. Solc, S. M. Dostaler, K. E. Neet, R. J. Riopelle, *J. Neurochem.* **2001**, *78*, 515.

[31] H. Irving, R. J. P. Williams, *J. Chem. Soc.* **1953**, 3192.

[32] W. C. Yount, D. M. Loveless, S. L. Craig, *Angew. Chem., Int. Ed.* **2005**, *44*, 2746.

[33] D. Mozhdehi, J. A. Neal, S. C. Grindy, Y. Cordeau, S. Ayala, N. Holten-Andersen, Z. Guan, *Macromolecules* **2016**, *49*, 6310.

[34] M. Maeder, Y.-M. Neuhold, *Practical Data Analysis in Chemistry*, Elsevier, Amsterdam **2007**.

[35] S. Sjöberg, *Pure Appl. Chem.* **1997**, *69*, 1549.

[36] J. D. Chai, M. Head-Gordon, *Phys. Chem. Chem. Phys.* **2008**, *10*, 6615.

[37] A. V. Marenich, C. J. Cramer, D. G. Truhlar, *J. Phys. Chem. B* **2009**, *113*, 6378.

[38] C. F. Quinn, M. C. Carpenter, M. L. Croteau, D. E. Wilcox, *Isothermal Titration Calorimetry Measurements of Metal Ions Binding to Proteins*, Elsevier Inc., Amsterdam **2016**.

[39] C. M. H. Ferreira, I. S. S. Pinto, E. V. Soares, H. M. V. M. Soares, *RSC Adv.* **2015**, *5*, 30989.

[40] A. Tripathi, K. C. Tam, G. H. McKinley, *Macromolecules* **2006**, *39*, 1981.

[41] F. Tanaka, S. F. Edwards, *J. Nonnewton. Fluid Mech.* **1992**, *43*, 247.

[42] F. Tanaka, S. F. Edwards, *J. Nonnewton. Fluid Mech.* **1992**, *43*, 289.

[43] M. Rubinstein, R. H. Colby, *Polymers Physics*, Oxford University Press, New York **2003**.

[44] L. M. Franklin, S. M. Walker, G. Hill, *J. Mol. Model.* **2020**, *26*, 116.

[45] L. Rulíšek, J. Vondrášek, *J. Inorg. Biochem.* **1998**, *71*, 115.

[46] D. Vaslensin, Ł. Szyrwiel, F. Camponeschi, M. Rowińska-Zyrek, E. Molteni, E. Jankowska, A. Szymanska, E. Gaggelli, G. Valensin, H. Kozłowski, *Inorg. Chem.* **2009**, *48*, 7330.

[47] J. H. Viles, F. E. Cohen, S. B. Prusiner, D. B. Goodin, P. E. Wright, H. J. Dyson, *Proc. Natl. Acad. Sci. U. S. A.* **1999**, *96*, 2042.

[48] P. Deschamps, P. P. Kulkarni, M. Gautam-Basak, B. Sarkar, *Coord. Chem. Rev.* **2005**, *249*, 895.

[49] P. Ferrer, F. Jiménez-Villacorta, J. Rubio-Zuazo, I. Da Silva, G. R. Castro, *J. Phys. Chem. B* **2014**, *118*, 2842.

[50] L. Zhou, S. Li, Y. Su, X. Yi, A. Zheng, F. Deng, *J. Phys. Chem. B* **2013**, *117*, 8954.

[51] A. Gergely, I. Sóvágó, *Inorg. Chim. Acta* **1976**, *20*, 19.

[52] M. Itabashi, K. Shoji, K. Itoh, *Inorg. Chem.* **1982**, *21*, 3484.

[53] Y. Altun, F. Köseoğlu, *J. Solution Chem.* **2005**, *34*, 213.

[54] T. Vander Hoogerstraete, N. R. Brooks, B. Norberg, J. Wouters, K. Van Hecke, L. Van Meervelt, K. Binnemans, *CrystEngComm* **2012**, *14*, 4902.

[55] T. Otieno, M. J. Hatfield, S. L. Asher, A. I. McMullin, B. O. Patrick, S. Parkin, *Synth. React. Inorg. Met. Chem.* **2001**, *31*, 1587.

[56] J. E. Bauman, J. C. Wang, *Inorg. Chem.* **1963**, *3*, 368.

[57] S. Tetteh, *Bioinorg. Chem. Appl.* **2018**, *2018*, 3157969.

[58] T. Dudev, C. Lim, *J. Am. Chem. Soc.* **2000**, *122*, 11146.

[59] R. R. Conry, in *Encyclopedia of Inorganic and Bioinorganic Chemistry*, (Ed: R. A. Scott), John Wiley & Sons, Ltd, Chichester, UK **2011**.

[60] R. R. Roe, Y.-P. Pang, *J. Mol. Model.* **1999**, *5*, 134.

[61] H. Keppler, in *Encyclopedia of Geochemistry*, (Eds: C. P. Marshall, R. W. Fairbridge), Springer, Berlin **1998**, pp. 118.

[62] S. A. Cazzell, N. Holten-Andersen, *Proc. Natl. Acad. Sci. U. S. A.* **2019**, *22*, 201906349.